ISSN: 0256-307X

中国物理快报

Chinese Physics Letters

Volume 30 Number 11 November 2013

A Series Journal of the Chinese Physical Society
Distributed by IOP Publishing

Online: http://iopscience.iop.org/0256-307X
http://cpl.iphy.ac.cn

CHINESE PHYSICAL SOCIETY
Institute of Physics PUBLISHING

CHIN. PHYS. LETT. Vol. 30, No. 11 (2013) 113401

High Gain Predictions for Ni-Like Ta Ions

Wessameldin S. Abdelaziz[1*], A. A. Farrag[2], H. M. Hamed[1], Mai E. Ahmed[3]

[1]*National Institute of Laser Enhanced Sciences, Cairo University, Giza, Egypt*
[2]*Faculty of Science, Cairo University, Giza, Egypt*
[3]*Environmental Affairs Agency (EEAA), Egypt*

(Received 5 July 2013)

Atomic structure data and effective collision strengths for $1s^2\ 2s^2\ 2p^6\ 3s^2\ 3p^6\ 3d^{10}$ and 54 fine-structure levels are contained in the configurations $1s^2\ 2s^2\ 2p^6\ 3s^2\ 3p^6\ 3d^9\ 4l$ $(l = s, p, d, f)$ for the nickel-like Ta ion. These data are used in the determination of the reduced population for the 55 fine structure levels over a wide range of electron densities (from 10^{21} to 10^{23}) and at various electron plasma temperatures. The gain coefficients for those transitions with a positive population inversion factor are determined and plotted against the electron density.

PACS: 34.80.Dp DOI: 10.1088/0256-307X/30/11/113401

Some experimental studies have tried to develop a high-efficiency x-ray laser with significant gain. For example, the researchers in Refs. [1,2] proposed the original mechanism for demonstrating x-ray lasing by resonant photo pumping. Several authors[3–8] have studied this lasing mechanism experimentally and theoretically in the hope of developing high-efficiency x-ray lasers.

In another study by Qi and Krishnan,[9] the shortest wavelength at which the significant gain has been measured using the resonant photo pumping was in the beryllium-like carbon at 2163 Å, which is far from the x-ray spectral region.

Nickel-like ions are of considerable interest in laser-plasma interaction because of the large gain in the extreme ultraviolet and x-ray regions. Their ground state $(1s^2\ 2s^2\ 2p^6\ 3s^2\ 3p^6\ 3d^{10}\ {}^1S_0)$ is analogous to the $(1s^2\ 2s^2\ 2p^6\ {}^1S_0)$ ground state of neon-like ions, which have already shown significant amplification in a number of elements such as selenium, germanium, and titanium. Similar laser gain has been predicted and observed by Goldstein *et al.*[10] in a number of nickel-like ions, including tin, neodymium, samarium, gadolinium, europium, tantalum, and tungsten.

Theoretical calculations are needed to approve these observations. Recently, Zhong *et al.*[11] calculated the energy levels, the spontaneous radiative decay rates, and the electron impact collisional strengths for Ni-like tantalum ions for the same defined 107 low lying fine-structure levels. However, no more works have been performed to predict the laser gain of Ni-like ions theoretically. In this Letter, we present the gain predicted for the Ni-like Ta ion by a steady-state model of Ni-like ions. Our model treats the kinetic of the Ni-like charge state in isolation from other ionization stages. The present gain calculations include the ground state $1s^2\ 2s^2\ 2p^6\ 3s^2\ 3p^6 3d^{10}$ and 54 fine-structure levels contained in the configurations $1s^2\ 2s^2\ 2p^6\ 3s^2\ 3p^6\ 3d^9\ 4l$ $(l = s, p, d, f)$ for the nickel-like Ta ion. The model includes all radiative transitions as well as electron-impact transitions among all levels.

The possibility of laser emission from plasma of the Ta^{45+} ion via electron collisional pumping in the XUV and soft x-ray spectral regions is investigated at different plasma temperatures and at different plasma electron densities.

The reduced population densities are calculated by solving the coupled rate equation[12–15]

$$N_j\Big[\sum_{i<j} A_{ij} + N_e\Big(\sum_{i<j} C^d_{ij} + \sum_{i>j} C^e_{ij}\Big)\Big] = N_e\Big(\sum_{i<j} N_i C^e_{ij} + \sum_{i>j} N_i C^d_{ij}\Big) + \sum_{i<j} N_i A_{ij}, \quad (1)$$

where N_j is the population of level j, A_{ji} is the spontaneous decay rate from level j to level i, C^e_{ji} is the electron collisional excitation rate coefficient, and C^d_{ji} is the electron collisional de-excitation rate coefficient, which is related to electron collisional excitation rate coefficient by[16,17]

$$C^d_{ji} = C^e_{ji}\Big[\frac{g_i}{g_j}\Big]\exp\Big[\frac{E_{ij}}{KT_e}\Big], \quad (2)$$

where g_i and g_j are the statistical weights of lower and upper levels, K is Boltzman's constant, T_e is the electron plasma temperature.

The electron impact excitation rates are usually expressed via the effective collision strengths γ_{ij} as

$$C^e_{ji} = \frac{8.6287\times10^{-6}}{g_i T_e^{1/2}}\gamma_{ij}\exp\Big[\frac{E_{ij}}{KT_e}\Big], \quad (3)$$

where C^e_{ji} is in units of cm^3/s, the values of γ_{ij} and A_{ji} can be taken from Ref. [10].

The actual population density N_j of the j^{th} level is obtained from the following identity[10]

$$N_j = N_j \times N_I, \quad (4)$$

*Corresponding author. Email: wessamlaser@yahoo.com

where N_I is the quantity of ions which reaches the ionization stage I, given by

$$N_I = \frac{f_I N_e}{Z_{\rm avg}}, \tag{5}$$

where f_I is the fractional abundance of the Ni-like ionization stages calculated by Goldstein *et al.*,[10] N_e is the electron density, and $Z_{\rm avg}$ is the average degree of ionization.

Since the populations calculated from Eq. (1) are normalized, we have

$$\sum_{j=1}^{55} \frac{N_j}{N_I} = 1, \tag{6}$$

where 55 is the number of all the levels of the ion under consideration, the quantity actually obtained from Eq. (1) is the fractional population N_j/N_I.

After the calculation of population of levels, the quantities N_u/g_u and N_l/g_l can be calculated. Application of electron collisional pumping, the collision in the laser ion plasma will transfer the pumped quanta to other levels, and will result in population inversions between the upper and lower levels. Once a population inversion has been ensured, a positive gain through $F > 0$ will be obtained.[18]

$$F = \frac{g_u}{N_u}\left[\frac{N_u}{g_u} - \frac{N_l}{g_l}\right], \tag{7}$$

where N_u/g_u and N_l/g_l are the reduced populations of the upper level and lower level, respectively. Equation (7) has been used to calculate the gain coefficient α for Doppler broadening of various transitions in the Ta^{45+} ion.

$$\alpha_{ul} = \frac{\lambda_{lu}^3}{8\pi}\left[\frac{M}{2\pi K T_i}\right]^{1/2} A_{ul} N_u F, \tag{8}$$

where M is the ion mass, T_i is the ion temperature in units of K, λ_{lu} is the transition wavelength in units of cm, u and l represent the upper and lower transition levels, respectively.

As seen from Eq. (8), the gain coefficient is expressed in terms of the upper state density N_u. N_u depends on how the upper state is populated, as well as on the density of the initial source state. The source state is often the ground state for the specific ion.

The reduced population densities are calculated for 55 fine structure levels arising from $1s^2\ 2s^2\ 2p^6\ 3s^2\ 3p^6\ 3d^{10}$ and 54 fine-structure levels contained in the configurations $1s^2\ 2s^2\ 2p^6\ 3s^2\ 3p^6\ 3d^9\ 4l$ ($l = s, p, d, f$) configurations that emit radiation in the XUV and soft x-ray spectral regions. The calculations are performed by solving the coupled rate Eq. (1) simultaneously using MATLAB version 7.3.0 computer program.

The present calculations for the reduced populations as a function of electron densities are shown in Figs. 1–3 at three different plasma temperatures (1, 1.5, 2.5 keV) for the Ta^{45+} ion.

In the calculation we take into account the spontaneous radiative decay rate and the electron collisional processes among all levels under study.

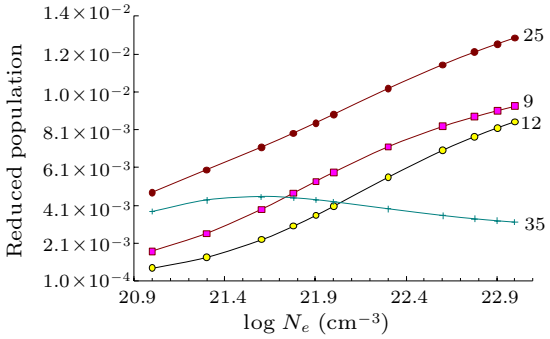

Fig. 1. Reduced population of Ta^{45+} levels after electron collisional pumping as a function of the electron density at temperature 1.0 keV.

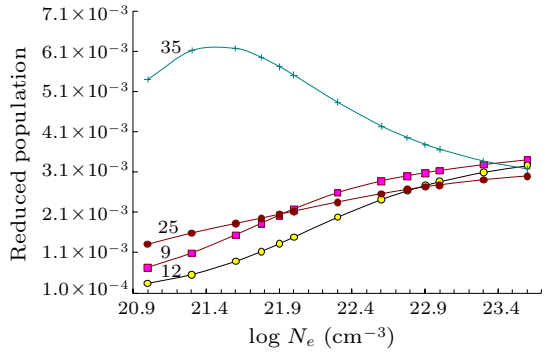

Fig. 2. Reduced population of Ta^{45+} levels after electron collisional pumping as a function of the electron density at temperature 1.5 keV.

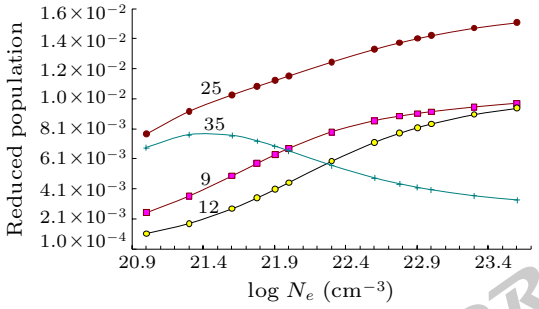

Fig. 3. Reduced population of Ta^{45+} levels after electron collisional pumping as a function of the electron density at temperature 2.5 keV.

The atomic structure data and effective collision strength data needed are taken from Ref. [11]. The behavior of level populations of the various ions can be explained as follows: in general at low electron densities the reduced population density is proportional to the electron density, where excitation to an excited state is followed immediately by radiative decay, and

collisional mixing of excited levels can be ignored.

The present result is in agreement with that of Feldman *et al.*[14–15,19] See also the data for nickel-like Sm, W, and Eu.[20–22] At high electron densities ($N_e > 10^{22}$), the radiative decay to all the levels will be negligible compared to collisional depopulations and all the level populations become independent of the electron density and are approximately equal (see Figs. 1–3). The $(3d_{3/2}\ 4d_{3/2})_0$ level shows a peak at electron density 4×10^{21} cm^{-3} before the other levels, then decreases to the saturation faster than the other levels, which means that the nonradiative transitions dominate the de-excitation because of its higher energy and fast decay time. The population inversion is largest, where electron collisional de-excitation rate for the upper level is comparable to radiative decay rate for this level.[14,19]

The lifetimes are determined almost entirely from the allowed and the strong intercombination transitions. The radiative lifetime of an excited atomic state u is related to the atomic transition probability by

$$\tau_u = \frac{1}{\sum A_{ul}}, \tag{9}$$

where the sum is taken over all the lower states which can be reached from the upper state by radiative decay.

Table 1 shows that the lifetime ratio between upper and lower laser levels 35/9 is 5, the ratio between 25/12 levels is 41, and the ratio between 35/12 is 10.6. The present calculations predict that the lifetime of the upper laser level must be longer than the lifetime of the lower one to ensure the fast depletion of the population of the lower level, which helps the laser to sustain continuous or quasi-continuous wave operation.

Table 1. The present results of radiative lifetime of the upper and lower laser levels for the nickel-like Ta.

Index	Level	Life time (ns)
9	$(3d_{3/2}\,4p_{1/2})_1$	1.91×10^{-4}
12	$(3d_{5/2}\,4p_{3/2})_1$	8.06×10^{-5}
25	$(3d_{5/2}\,4d_{5/2})_2$	3.31×10^{-3}
35	$(3d_{3/2}\,4d_{3/2})_0$	8.56×10^{-4}

The reduced populations obtained above are very important for gain calculations. In order to work in the XUV and x-ray spectral regions, we have chosen transitions between any two levels producing photons with wavelengths between 30 Å and 150 Å.

The population inversion is largest where the electron collisional de-excitation rate for the upper level is comparable to the radiative decay rate for this level. For example, the population inversion factor for the 35→9 transition at $N_e = 10^{21}$ cm^{-3} is equal to 0.88 at 2500 eV for Ta^{45+}.

As a result of population inversion there will be positive gain in laser medium. Equation (8) has been used to calculate the gain coefficient for the Doppler broadening of various transitions in the Ta^{45+} ion. Our results for the maximum gain coefficient in cm^{-1} for those transitions have a positive inversion factor $F > 0$ in the case of Ta^{45+}, as shown in Figs. 4–6.

The figures show that the population inversions occur for several transitions in the Ta^{45+} ion. However, the largest gain occurs for the Ta^{45+} ion in the $(3d_{3/2}\ 4d_{3/2})_0 \rightarrow (3d_{3/2}\ 4p_{1/2})_1$ (35→9) transition at wavelength 45 Å at electron temperatures of 1000, 1500, and 2500 eV.

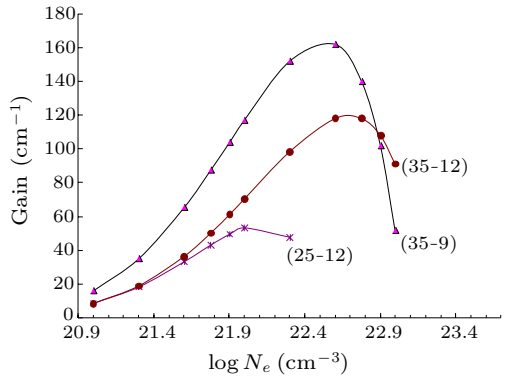

Fig. 4. Gain coefficient of possible laser transitions against electron density at temperature 1 keV in Ta^{45+}.

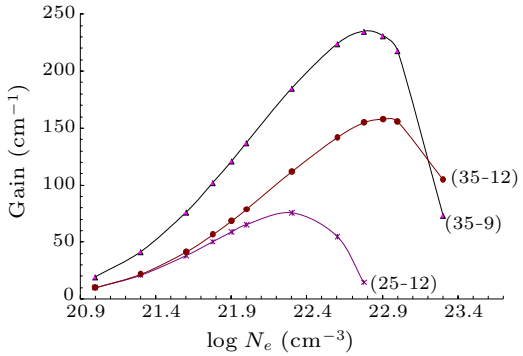

Fig. 5. Gain coefficient of possible laser transitions against electron density at temperature 1.5 keV in Ta^{45+}.

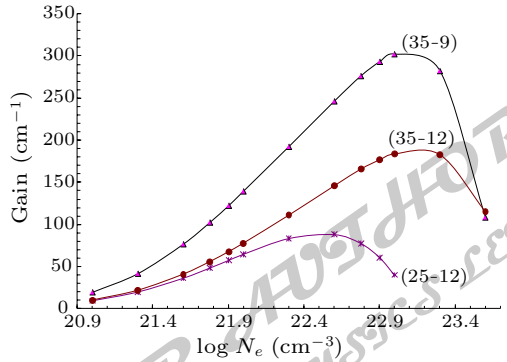

Fig. 6. Gain coefficient of possible laser transitions against electron density at temperature 2.5 keV in Ta^{45+}.

For Ni-like ions, the population inversion is due

to strong monopole excitation from the $3d^{10}$ ground state to the $3d^9 4d$ configuration, and also the radiative decay of the $3d^9 4d$ level to the ground level is forbidden, while the $3d^9 4p$ level decays very rapidly to the ground level.

This short-wavelength laser transition is produced using plasmas created by optical lasers as the lasing medium. For electron densities and electron temperatures that are typical characteristics of laboratory high-density plasma sources, such as laser produced plasmas, it is possible to create a quasistationary population inversion between the $3d^9 4d$ and $3d^9 4p$ in the Ta^{45+} ion. Our calculations have shown that, under favorable conditions, large laser gains for this transition in the XUV and soft x-ray regions of the spectrum can be achieved in the nickel-like Ta ion. It is obvious that the gain increases with the temperature. For the Ta^{45+} ion, Chen and Osterheld[23] predicted the same three laser transitions, which are also predicted by us but they assumed that electron and ion temperatures are identical and made their calculations at constant ion densities (2×10^{19} and $2 \times 10^{20}\,\mathrm{cm}^{-3}$).

Table 2. Parameters of the most intense laser transitions, i.e., wavelength λ, maximum gain α, electron density N_e, and electron temperature T_e.

Transition	λ (Å)	α (cm^{-1})	N_e (cm^{-3})	T_e (keV)
$(3d_{3/2}\,4d_{3/2})_0 \rightarrow (3d_{3/2}\,4p_{1/2})_1$	45	302	1×10^{23}	2.5
$(3d_{5/2}\,4d_{5/2})_2 \rightarrow (3d_{5/2}\,4p_{3/2})_1$	75.6	88	4×10^{22}	2.5
$(3d_{3/2}\,4d_{3/2})_0 \rightarrow (3d_{5/2}4p_{3/2})_1$	51.5	184	1×10^{23}	2.5

In summary, we have presented an analysis to show that electron collisional pumping (ECP) is suitable for attaining population inversion and for offering the potential for laser emission in the spectral region between 50 and 150 Å from Ta^{45+} ions. This class of lasers can be achieved under suitable conditions of pumping power as well as electron density. If the positive gains obtained previously for some transitions in the ions under studies (Ta^{45+} ion) together with the calculated parameters could be achieved experimentally, then successful low-cost electron collisional pumping XUV and soft x-ray lasers can be developed for various applications. The parameters of most intense laser transitions in Ni-like La ions are summarized in Table 2.

References

[1] Vinogradov A V, Sobelman I I and Yukov E A 1975 *Sov. J. Quantum Electron.* **5** 59
[2] Norton B A and Peacock N J 1975 *J. Phys.* B **8** 989
[3] Bhagavatula V A 1976 *J. Appl. Phys.* **47** 4535
[4] Monier P, Chenais-Popovics C, Geindre J P and Gauthier J C 1988 *Phys. Rev.* A **38** 2508
[5] Nilsen J 1991 *Phys. Rev. Lett.* **66** 305
[6] Porter J L, Spielman R B, Matzen M K, McGuire E J, Ruggles L E, Vargas M F, Apruzese J P, Clark R W and Davis J 1992 *Phys. Rev. Lett.* **68** 796
[7] Zhang J and Fill E E 1992 *Opt. Quantum Electron.* **24** 1343
[8] Nilsen J, Beiersdorfer P, Elliott S R, Phillips T W, Bryunetkin B A, Dyakin V M, Pikuz T A, Faenov A Ya, Pikuz S A, von Goeler S, Bitter M, Loboda P A, Lykov V A and Politov V Yu 1994 *Phys. Rev.* A **50** 2143
[9] Qi N and Krishnan M 1987 *Phys. Rev. Lett.* **59** 2051
[10] Goldstein W H, Oreg J, Zigler A, Bar-Shalom A and Klapisch M 1988 *Phys. Rev.* A **38** 1797
[11] Zhong J Y, Zahng J, Zeng J L, Zhao G and Gu M F 2005 *At. Data Nucl. Data Tables* **89** 101
[12] Feldman U, Bhatia A K and Suckewer S 1983 *J. Appl. Phys.* **45** 2188
[13] Feldman U, Seely J F and Doschek G A 1986 *J. Appl. Phys.* **59** 3953
[14] Feldman U, Doschek G A, Seely J F and Bhatia A K 1985 *J. Appl. Phys.* **58** 2909
[15] Feldman U, Seely J F and Bhatia A K 1984 *J. Appl. Phys.* **56** 2475
[16] Chapline G and Wood L 1975 *Phys. Today* **28** 40
[17] Vinogradov A V and Shlyaptsev V N 1980 *Sov. J. Quantum Electron.* **10** 754
[18] Sobel'man I I 1979 *Introduction to the Theory of Atomic Spectra, International Series of Monographs in Natural Philosophy* (Oxford: Pergamon Press) vol 40
[19] Feldman U, Seely J F and Bhatia A K 1985 *J. Appl. Phys.* **58** 3954
[20] Abdelaziz W S 2009 *Phys. Scr.* **79** 1
[21] Abdelaziz W S 2009 *Eur. Phys. J.* D **75** 17
[22] Abdelaziz W S and El Sherbini 2010 *Opt. Laser Technol.* **42** 699
[23] Chen M H and Osterheld A L 1995 *Phys. Rev.* A **52** 3790

Chinese Physics Letters

Volume 30 Number 11 November 2013

GENERAL

110201 A Fractional-Order Phase-Locked Loop with Time-Delay and Its Hopf Bifurcation
YU Ya-Juan, WANG Zai-Hua

110202 CTE Solvability and Exact Solution to the Broer-Kaup System
CHEN Chun-Li, LOU Sen-Yue

110301 Analytical Arbitrary-Wave Solutions of the Deformed Hyperbolic Eckart Potential by the Nikiforov–Uvarov Method
ZHANG Min-Cang

110302 Impact of Cross-Phase Modulation Induced by Classical Channels on the CV-QKD in a Hybrid System
CHEN Yan, SHEN Yong, TANG Guang-Zhao, ZOU Hong-Xin

110303 Radio-Frequency Spectra of Ultracold Fermi Gases Including a Generalized GMB Approximation at Unitarity
RUAN Xiao-Xia, GONG Hao, DU Long, JIANG Yu, SUN Wei-Min, ZONG Hong-Shi

110304 Unraveling a Driven Damped Harmonic Oscillator through Entangled State Representation
Seyed Mahmoud Ashrafi, Mohammad Reza Bazrafkan

110305 Dynamics of Dark Solitons in Superfluid Fermi Gases
QI Xiu-Ying, ZHANG Ai-Xia, XUE Ju-Kui

110501 Enhancement of Localization in a Driven Four-Well System with Second-Order Coupling
LI Li-Ping, LUO Xiao-Bing, HU Qiang-Lin, YU Xiao-Guang

110502 Transition Mode of Two Parallel Flags in Uniform Flow
WANG Si-Ying, DUAN Wen-Gang, YIN Xie-Zhen

110503 Semi-physical Simulation Platform of a Parafoil Nonlinear Dynamic System
GAO Hai-Tao, YANG Sheng-Bo, ZHU Er-Lin, SUN Qing-Lin, CHEN Zeng-Qiang, KANG Xiao-Feng

110504 An Exact Numerical Approach to Calculate the First Passage Time for General Random Walks on a Network
XIE Yan-Bo, LI Yu-Jian, LI Ming, XI Zhen-Dong, WANG Bing-Hong

110505 Kernel Least Mean Kurtosis Based Online Chaotic Time Series Prediction
QU Hua, MA Wen-Tao, ZHAO Ji-Hong, CHEN Ba-Dong

110506 Dynamical Behaviors of a TiO_2 Memristor Oscillator
WANG Guang-Yi, HE Jie-Ling, YUAN Fang, PENG Cun-Jian

THE PHYSICS OF ELEMENTARY PARTICLES AND FIELDS

111101 A Lattice Non-Perturbative Definition of an $SO(10)$ Chiral Gauge Theory and Its Induced Standard Model
WEN Xiao-Gang

111201 Electron-Positron Pair Creation from Vacuum by using Negative Frequency Chirping Laser Pulses
SANG Hai-Bo, JIANG Min, XIE Bai-Song

111202 Complete Analyses on the Short-Distance Contribution of $B_s \to \ell^+\ell^-\gamma$ in the Standard Model
WANG Wen-Yu, XIONG Zhao-Hua, ZHOU Si-Hong

NUCLEAR PHYSICS

112101 Lifetime Measurement of the Low Lying Yrast States in ^{189}Pt
HE Chuang-Ye, WU Xiao-Guang, WANG Jin-Long, WU Yi-Heng, ZHENG Yun, LI Guang-Sheng, LI Cong-Bo, HU Shi-Peng, LI Hong-Wei, LIU Jia-Jian, LUO Peng-Wei, YAO Shun-He

ATOMIC AND MOLECULAR PHYSICS

113101 Theoretical Study of the H+ClO Reaction
LI Ya-Min, CHE Ru-Xin, LI Ying, DONG Bin

113301 **Ionization Channels of the Molecular Ion H_2^+ in Intense Laser Field**
MIAO Xiang-Yang, SHI Hao-Ting

113302 **Manipulation of Resonance-Enhanced Multiphoton-Ionization Photoelectron Spectroscopy by Two Time-Delayed Femtosecond Laser Pulses**
LU Chen-Hui, ZHANG Shi-An, SUN Zhen-Rong

113401 **High Gain Predictions for Ni-Like Ta Ions**
Wessameldin S. Abdelaziz, A. A. Farrag, H. M. Hamed, Mai E. Ahmed

113402 **Molecular Dynamics Simulation of Damage to Coiled Carbon Nanotubes under C Ion Irradiation**
ZHOU Bin, ZHANG Wei, GONG Wen-Bin, WANG Song, REN Cui-Lan, WANG Cheng-Bin, ZHU Zhi-Yuan, HUAI Ping

FUNDAMENTAL AREAS OF PHENOMENOLOGY(INCLUDING APPLICATIONS)

114201 **Tunable and Linewidth-Reduced Laser Diode Stack for Rubidium Laser Pumping**
LI Zhi-Yong, TAN Rong-Qing, XU Cheng, LI Lin

114202 **Fabrication and Characterization of High Power 1064-nm DFB Lasers**
TAN Shao-Yang, ZHAI Teng, LU Dan, WANG Wei, ZHANG Rui-Kang, JI Chen

114203 **Vacuum Rabi Splitting and Dynamics of the Jaynes–Cummings Model for Arbitrary Coupling**
ZHANG Yu-Yu, CHEN Qing-Hu, ZHU Shi-Yao

114204 **Nanosecond Pulse Generation Using the Stimulated Brillouin Scattering Effect in a Photonic Crystal Fiber**
Z. Jusoh, N. S. Shahabuddin, N. M. Ali, H. Ahmad, S. W. Harun

114205 **Carrier-Envelope-Phase Control of Single-Electron Transport in Coupled Quantum Dots**
YANG Wen-Xing, CHEN Ai-Xi, BAI Yan-Feng, LU Jia-Wei

114206 **Compact and Tunable Mid-IR Light Source Based on a Dual-Wavelength Fiber Laser**
CHANG Jian-Hua, WANG Ting-Ting, ZHANG Chuang, GE Yi-Xian, TAO Zai-Hong

114207 **Quantum Random Number Generation Based on Quantum Phase Noise**
TANG Guang-Zhao, JIANG Mu-Sheng, SUN Shi-Hai, MA Xiang-Chun, LI Chun-Yan, LIANG Lin-Mei

114208 **Generation of Optical Accelerating Quinary-Cusp Beams and Their Optical Characteristics**
REN Zhi-Jun, LI Xiao-Dong, FAN Chang-Jiang, XU Zhuo-Qi

114209 **A 300-MHz Bandwidth Balanced Homodyne Detector for Continuous Variable Quantum Key Distribution**
HUANG Duan, FANG Jian, WANG Chao, HUANG Peng, ZENG Gui-Hua

114301 **Three-Dimensional Sound Propagation and Scattering in Two-Dimensional Waveguides**
QIN Ji-Xing, LUO Wen-Yu, ZHANG Ren-He, YANG Chun-Mei

114401 **Simulation of Radiative Transfer in Nonequilibrium Plasmas Containing N and O Species Based on the Approximate Collision-Radiative Method**
HE Xin, CHANG Sheng-Li, DAI Sui-An, YANG Jun-Cai

PHYSICS OF GASES, PLASMAS, AND ELECTRIC DISCHARGES

115201 **Cluster Rotation in an Unmagnetized Dusty Plasma**
HUANG Feng, LIU Yan-Hong, CHEN Zhao-Yang, WANG Long, YE Mao-Fu

CONDENSED MATTER: STRUCTURE, MECHANICAL AND THERMAL PROPERTIES

116201 **Tensile Strength of Zr–Ti Binary Alloy**
ZHOU Yun-Kai, JING Ran, MA Ming-Zhen, LIU Ri-Ping

116501 **Path Integral Monte Carlo Study of X@C_{50} [X=H_2, He, Ne, Ar]**
PENG Chun, ZHANG Hong, CHENG Xin-Lu

116801 Unintentional Doping Mechanisms in GaAs/Si Films Grown by Metalorganic Chemical Vapor Deposition
WANG Jun, DENG Can, JIA Zhi-Gang, WANG Yi-Fan, WANG Qi, HUANG Yong-Qing, REN Xiao-Min

CONDENSED MATTER: ELECTRONIC STRUCTURE, ELECTRICAL, MAGNETIC, AND OPTICAL PROPERTIES

117101 First Principles Study on the Stability and Mechanical Properties of MB (M=V, Nb and Ta) Compounds
QI Chen-Jin, FENG Jing, ZHOU Rong-Feng, JIANG Ye-Hua, ZHOU Rong

117102 A Comparative Study of Ballistic Transport Models for Nanowire MOSFETs
ZHANG Li-Ning, MEI Jin-He, ZHANG Xiang-Yu, TAO Jin, HU Yue, HE Jin, CHAN Mansun

117103 Electronic States of $IC_{60}BA$ and $PC_{71}BM$
SHENG Chun-Qi, WANG Peng, SHEN Ying, LI Wen-Jie, ZHANG Wen-Hua, ZHU Jun-Fa, LAI Guo-Qiao, LI Hong-Nian

117104 Degradation Characteristics of Resistive Switching Memory Devices Correlated with Electric Field Induced Ion-Migration Effect of Anode
LIU Rui, QIU Gang, CHEN Bing, GAO Bin, KANG Jin-Feng

117201 Electrical Characterization in the Phase Transition between Cubic $PbCrO_3$ Perovskites at High Pressures
WANG Wen-Dan, HE Duan-Wei, XIAO Wan-Sheng, WANG Shan-Min, XU Ji-An

117301 Vacuum Violet Photo-Response of AlGaN-Based Metal-Semiconductor-Metal Photodetectors
ZHOU Dong, LU Hai, CHEN Dun-Jun, REN Fang-Fang, ZHANG Rong, ZHENG You-Dou, LI Liang

117801 Enhanced Crystalization and Sensitization of Si Nanocrystals in Al_2O_3:Er/Si:Er Multilayers
WANG Jun-Zhuan, YANG Xin-Xin, WEI Xiao-Xu, YU Lin-Wei, SHI Yi

117802 Raman Gain Coefficients of Nd:$Lu_xY_{1-x}VO_4$ Crystals
ZHANG Fang, WANG Zheng-Ping, ZHAO Yong-Guang, XU Xin-Guang

117901 Strain-Sensitive Current-Voltage Characteristics of ZnSe Nanowire in Metal-Semiconductor-Metal Nanostructure
TAN Yu, WANG Yan-Guo

CROSS-DISCIPLINARY PHYSICS AND RELATED AREAS OF SCIENCE AND TECHNOLOGY

118101 Fabrication and Photostability of Rhodamine-6G Gold Nanoparticle Doped Polymer Optical Fiber
Suneetha Sebastian, Ajina C, C. P. G Vallabhan, V. P. N. Nampoori, P. Radhakrishnan, M. Kailasnath

118102 Broadband Light Emission from Chirped Multiple InAs Quantum Dot Structure
LV Xue-Qin, JIN Peng, CHEN Hong-Mei, WU Yan-Hua, WANG Fei-Fei, WANG Zhan-Guo

118103 Upconversion Properties of the Er-Doped Y_2O_3, Bi_2O_3 and Sb_2O_3 Nanoparticles Fabricated by Pulsed Laser Ablation in Liquid Media
Reza Zamiri, Hamid-Reza Bahari-Poor, Azmi Zakaria, Raheleh Jorfi, Golnoush Zamiri, Avito Rebelo, Akrajas Ali Omar

118201 Measurement of ZnO/Al_2O_3 Heterojunction Band Offsets by *in situ* X-Ray Photoelectron Spectroscopy
LEI Hong-Wen, ZHANG Hong, WANG Xue-Min, ZHAO Yan, YAN Da-Wei, JIANG Zhong-Qian, YAO Gang, ZENG Ti-Xian, WU Wei-Dong

118501 Strained Germanium-Tin pMOSFET Fabricated on a Silicon-on-Insulator Substrate with Relaxed Ge Buffer
SU Shao-Jian, HAN Gen-Quan, ZHANG Dong-Liang, ZHANG Guang-Ze, XUE Chun-Lai, WANG Qi-Ming, CHENG Bu-Wen

118701 Quantifying the Attractive Force Exerted on the Pinned Calcium Spiral Waves by Using the Adventive Field
QIU Kang, TANG Jun, LUO Jin-Ming, MA Jun

118702 Effect of Low-Pass Filtering in Force Calibration of Magnetic Tweezers
ZHENG Hai-Zi, NONG Da-Guan, LI Ming

118801 Efficient Natural Dye-Sensitized Solar Cells Based on Spin-Coated TiO_2 Anode Materials
YU Xiao-Hong, SUN Zhao-Zong, LIAN Jie, LI Yi-Tan, CHEN Yan-Xue, GAO Shang, WANG Xiao, WANG Ying-Shun, ZHAO Ming-Lin

118901 Long-Term Effects of Recommendation on the Evolution of Online Systems
ZHAO Dan-Dan, ZENG An, SHANG Ming-Sheng, GAO Jian

GEOPHYSICS, ASTRONOMY, AND ASTROPHYSICS

119801 Cosmology with an Effective Λ-Term in Lyra Manifold
V. K. Shchigolev

ERRATA AND OTHER CORRECTIONS

119901 Erratum: Pulsar Timing Residuals Induced by Gravitational Waves from Single Non-evolving Supermassive Black Hole Binaries with Elliptical Orbits [Chin. Phys. Lett. 30 (2013) 100402]
TONG Ming-Lei, YAN Bao-Rong, ZHAO Cheng-Shi, YIN Dong-Shang, ZHAO Shu-Hong, YANG Ting-Gao, GAO Yu-Ping